

# Geophysical Research Letters®



## RESEARCH LETTER

10.1029/2024GL109601

### Key Points:

- Forecast and analysis errors within dry intrusions (DIs) above the Azores are studied using data assimilation (DA) output
- DIs and the boundary layer beneath exhibit a cold bias and near-surface wind and humidity underestimation
- Low-level wind speed and humidity biases are not reduced through DA with possible implications for midlatitude weather

### Supporting Information:

Supporting Information may be found in the online version of this article.

### Correspondence to:

A. Schäfler,  
[andreas.schaeffler@dlr.de](mailto:andreas.schaeffler@dlr.de)

### Citation:

Schäfler, A., Krüger, K., Oertel, A., Quinting, J. F., & Raveh-Rubin, S. (2024). Indication for biases in dry intrusions and the marine boundary layer over the Azores in ECMWF short-term forecasts and analyses. *Geophysical Research Letters*, 51, e2024GL109601. <https://doi.org/10.1029/2024GL109601>

Received 2 APR 2024

Accepted 17 JUL 2024

© 2024. The Author(s).

This is an open access article under the terms of the [Creative Commons Attribution License](#), which permits use, distribution and reproduction in any medium, provided the original work is properly cited.

## Indication for Biases in Dry Intrusions and the Marine Boundary Layer Over the Azores in ECMWF Short-Term Forecasts and Analyses

A. Schäfler<sup>1</sup> , K. Krüger<sup>1</sup> , A. Oertel<sup>2</sup> , J. F. Quinting<sup>2</sup> , and S. Raveh-Rubin<sup>3</sup> 

<sup>1</sup>Deutsches Zentrum für Luft- und Raumfahrt (DLR), Institut für Physik der Atmosphäre, Oberpfaffenhofen, Germany,

<sup>2</sup>Institute of Meteorology and Climate Research, Troposphere Research (IMKTRO), Karlsruhe Institute of Technology (KIT), Karlsruhe, Germany, <sup>3</sup>Department of Earth and Planetary Sciences, Weizmann Institute of Science, Rehovot, Israel

**Abstract** The model representation of dry intrusions (DIs) and the marine boundary layer (MBL) is analyzed in the European Centre for Medium-Range Weather Forecasts (ECMWF) Integrated Forecasting System (IFS). For this purpose, a DI classification at the Azores is combined with observation, short-term background forecast and analysis data from the IFS data assimilation system. The background exhibits a cold bias in the descending DI, which is possibly related to a cold bias in the MBL below through vertical mixing. At the surface, simulated wind speeds are underestimated and directions are veered compared to the observations. The errors are reduced in the analysis except for near-surface wind and humidity biases. We hypothesize that these biases are connected through underestimated surface latent heat fluxes. Such persistent biases potentially influence local weather and midlatitude weather evolution as cyclones are supplied with moisture from the cold sector influenced by DIs.

**Plain Language Summary** The representation of descending dry intrusion airstreams and the marine boundary layer at the Azores is investigated in a global numerical weather prediction model. Specifically, radiosonde observations are compared with short-term forecast and analysis data to identify biases. The diagnosed underestimated temperature, specific humidity, and wind speed in the lower troposphere are important as they can influence the evolution of mid-latitude weather.

## 1. Introduction

Dry intrusions (DIs) are slantwise descending synoptic-scale air streams that transport air from the upper troposphere and, less frequently, from the lower stratosphere equatorward and downward toward and often into the planetary boundary layer (PBL) (Browning, 1997; Carlson, 1980). The DI air, which spreads out behind the cold front in the cold sector of an extratropical cyclone, typically originates from the eastern side of an upper-level ridge from where it coherently descends on the rear of a downstream trough. The descending air becomes more humid due to mixing with moist PBL air beneath. In the PBL, this mixing enhances near-surface temperature and moisture deficits and, thus, turbulent fluxes (Raveh-Rubin, 2017), especially over oceans where DIs are most frequent. Strong upward directed surface latent heat fluxes in cold polar air advected over warm ocean surfaces (e.g., Aemisegger & Papritz, 2018) can supply moisture to subsequent midlatitude cyclones (Boutle et al., 2010; Papritz et al., 2021; Sodemann & Stohl, 2013; Wenta et al., 2024) and influence the cyclone strength and related precipitation (Dacre et al., 2019; Demirdjian et al., 2023). In addition, advection of cyclonic potential vorticity in DIs originating in the stratosphere can lead to an intensification of the cyclones in which DIs are embedded (Uccellini et al., 1985; Young et al., 1987). And, DIs may increase convective activity (Russell et al., 2009, 2012), precipitation ahead of the cold front (e.g., Raveh-Rubin & Wernli, 2016) and severe surface wind gusts through facilitating transport of high momentum (Givon et al., 2024; Raveh-Rubin & Wernli, 2015).

Despite their importance for the evolution of midlatitude cyclones, little is known about the representation of DIs in numerical weather prediction (NWP) models. Descending stratospheric air is mixed with surrounding tropospheric air masses (e.g., Schäfler et al., 2023), a process that is believed to be misrepresented in current NWP models (Krüger et al., 2022). Beneath the DI, sub-grid scale processes determine the PBL structure and composition, which are parameterized in models (Teixeira et al., 2008) and are a possible cause of systematic errors (Frassoni et al., 2023). Near-surface wind errors are one of the most long-lasting model biases (Brown et al., 2005, 2006; Hollingsworth, 1994) that, although having somewhat decreased over the past years, still affect

recent NWP forecasting systems (Belmonte Rivas & Stoffelen, 2019; Sandu et al., 2020; Savazzi et al., 2022). Over midlatitude oceans the mean wind direction is underestimated (too northerly), zonal wind speeds overestimated and meridional wind speeds underestimated. These low-level errors were related to situations with high stability in the marine boundary layer (MBL), as typical for warm air advection in the warm sector of cyclones, showing highest wind direction errors. Similar but smaller errors are observed in unstable, convective MBLs that were associated with insufficient turbulent momentum transport (Brown et al., 2005, 2006), to which the destabilizing effect of DIs (Raveh-Rubin, 2017) may contribute. Sandu et al. (2020) show that unstable MBLs, which are more frequent than stable ones, contribute more to the average wind errors. Due to the importance of winds for the strength of turbulent fluxes, such wind errors may also affect temperature and humidity structure in the MBL. Schäfler et al. (2011) find a moist bias in the inflow of a warm conveyor belt, which they linked to misrepresented surface fluxes over land. In contrast, Lavers et al. (2020) find a dry bias below 850 hPa accompanied by a slow wind speed bias near the surface during warm air advection situations related to atmospheric rivers over the Pacific Ocean. These situations were also characterized by a cold bias throughout the troposphere.

In this study, the representation of vertical profiles of wind, temperature and humidity in DI situations is investigated in the European Centre for Medium-Range Weather Forecasts (ECMWF) Integrated Forecasting System (IFS). The Azores, due to their remote location in the eastern North Atlantic, within a region of climatologically high DI occurrence, are one of the rare locations with operational profile observations of DIs interacting with the MBL. Radiosonde data of three winter months (DJF) in the years 2016–2018 showed a typical sequence of events for DIs (Ilotoviz et al., 2021) consisting of (a) a pre-DI cold front phase, (b) the DI event and (c) a post-DI recovery phase. The average vertical profiles for these phases significantly differ from the usual Non-DI distributions. We extend the work by Ilotoviz et al. (2021) and combine their DI classification with direct output from ECMWF's DA system (ECMWF, 2016a; Rabier et al., 2000) to compare observations and their model equivalents. Such DA output is used to diagnose systematic model biases globally (e.g., Sandu et al., 2020) but also related to individual processes or regions (Krüger et al., 2022; Lavers et al., 2018, 2023). We address the following questions: (a) How well are DIs and the MBL at the Azores represented in the ECMWF IFS? (b) What is the impact of DA on the structure of the DI and the MBL in the analysis?

## 2. Data and Methods

Ilotoviz et al. (2021) used 1073 radiosondes from the Atmospheric Radiation Measurements site on the island of Graciosa (39.1°N, 28°W, WMO ID: 08507), Azores, Portugal in the DJF months from 2016 to 2018. The Graciosa radiosonde data, with profiles every 12 hr (partially 6 hourly), are not made available for DA. However, radiosondes launched from the station at Lajes (38.8°N, 27.1°W, WMO ID: 08508) on the island of Terceira, Azores, Portugal at 12 UTC were operationally assimilated at ECMWF during the same period. The DA system creates the most accurate gridded representation of the atmospheric state (analysis) by blending a short-term forecast (background) with observations. In total, 256 quality-controlled radiosonde profiles of temperature, wind and humidity in pressure coordinates are used for assimilation. Besides these observations, departures of the background forecast (also referred to as first guess departures or innovations) and the analysis (analysis departure, residual) from the observations are provided. Spatial and temporal interpolation of gridded model fields to the observation locations is done within the DA system. For the presented analysis the irregularly distributed data is interpolated to a common vertical pressure grid. Here, equidistant levels in the logarithm of pressure (approx. constant altitude grid of 180 m) are used.

The 256 radiosondes at Lajes are categorized using the DI classification for Graciosa (Ilotoviz et al., 2021), which is considered feasible as the two stations are only 90 km apart and DI outflows typically extend over several hundred kilometers in latitude and longitude (Raveh-Rubin, 2017). DI events are identified whenever globally initiated air mass trajectories, which fulfill a minimum descent criterion of 400 hPa in 48 hr, reach into a 1° radius around the station and their pressure is >700 hPa. The DI is followed by a 24 hr post-DI phase. A cold front detection and DI-matching scheme (Catto & Raveh-Rubin, 2019) is applied to identify Pre-DI fronts and to distinguish Non-DI situations with and without fronts. The five classes and their frequency for the Graciosa and Lajes profile time steps are compared in Table 1. Although the 24-hourly Lajes data contains only 24% of the Graciosa time steps, the share of DIs is relatively similar (5.9% and 7.8%). The relative share of all DI classes (Pre-DI, DI and Post-DI) is 21% at Graciosa and 16% at Lajes. Text S1 and Figures S1–S3 in Supporting Information S1 provide more information about the data availability.

**Table 1**

*Number of Radiosonde Profiles at the Stations Graciosa and Lajes, Azores, Portugal per Class*

Class	Number of profiles at Graciosa (% of time)	Number of profiles at Lajes (% of time)
Non-DIs	649 (60.5)	194 (75.8)
Non-DIs fronts	196 (18.3)	20 (7.8)
Pre-DIs fronts	91 (8.9)	8 (3.1)
DIs	63 (5.9)	20 (7.8)
Post-DIs	74 (6.9)	14 (5.5)
Total	1,073 (100)	256 (100)

### 3. Results and Discussion

#### 3.1. Mean Vertical Profiles

Figure 1 shows average vertical profiles of temperature, specific humidity and wind per class. DIs are preceded by a pre-DI cold front phase, that is, the warm sector of a cyclone, with anomalously high temperatures (Figure 1a) and humidity (Figure 1b). In addition, the pre-DI phase is characterized by thick clouds (not shown) and increased southwesterly low-level winds (Figures 1c and 1d). Behind the front, winds turn northerly, advecting cold and dry MBL air. Accordingly, the DI class exhibits the coldest temperatures at almost all altitudes up to 500 hPa. Above the mixed layer (ML), defined as the surface-based layer with a dry adiabatic lapse rate up to 925 hPa (see constant potential temperature in Figure S4a in Supporting Information S1), a nearly dry adiabatic and, thus, weakly stable layer extends up to 870 hPa. This decoupled layer (DL) is typical for post-cold-frontal regions (Kazemirad & Miller, 2020; Wood, 2012). Beyond the DL, an inversion layer (IL) up to 790 hPa is formed by the near-surface cold air advection strengthened by DI air entering the MBL. Specific humidity is almost constant in the ML ( $\sim 5.8 \text{ g kg}^{-1}$ ; Figure 1b) and gently declines in the DL due to mixing with dry air above. The mixing reduces stability and favors a thick, well-mixed convective MBL in the cyclone's cold sector (see vertically decreasing equivalent potential temperature in Figure S4b in Supporting Information S1). Above the DL, a strong vertical humidity gradient occurs across the IL with specific humidity  $< 1 \text{ g kg}^{-1}$  in the free tropospheric DI air. Horizontal wind is almost constant in speed ( $\sim 12 \text{ m s}^{-1}$ ) and direction ( $\sim 335^\circ$ ; Figure 1c) in the ML. Above, horizontal wind speed constantly increases, and the DIs possess the highest wind speeds of all classes above 800 hPa with north-westerly directions. The backing of winds with increasing altitude (anticlockwise) is related to the strong cold advection below 650 hPa and contrasts the usual veering winds in the MBL. During the post-DI phase, the influence of strong surface heat and moisture fluxes can be seen from the warming and recovery of moisture in the MBL. Wind directions turn westerly and wind speeds are lower compared to the DI class. The DI and post-DI phase strongly differ from the average conditions represented by the Non-DI and frontal classes. Specifically, the MBL is much colder and drier, DI wind speed is increased compared to the average wind speed and wind directions differ from the usual southwesterly flow. The latter is related to the Azores' usual location in the northeastern quadrant of the subtropical anticyclone and at some distance to the waveguide explaining the overall weak wind speeds at all altitudes. Although the data set provides a lower number of DI events, the vertical profiles are very similar to Ilotoviz et al. (2021).

#### 3.2. Background Departures

To identify potential model biases, we next consider the departure of the model background from the observation (innovation). Figure 2 shows the median departures of the observations (Figure 1) from the background forecasts for all classes and variables. The Non-DI class, which represents the climatological average conditions, exhibits a cold bias (i.e., positive innovation) from the surface up to the mid troposphere of  $\sim 0.2 \text{ K}$  (Figure 2a). The DI class shows the highest positive temperature innovations (0.7–1.0 K) in the layer from  $\sim 700$  to 850 hPa equivalent to a cold bias in the descending air. Beneath the IL, the cold bias extends into the MBL with smaller but still enhanced values of  $\sim 0.5 \text{ K}$ , which is possibly influenced by mixing with the biased DI air above. The post-DI class, following the DI event, exhibits a substantial cold bias below 850 hPa, which is potentially also related to the DI cold bias and subsequent mixing into the MBL. Although temperature innovations of the frontal classes (pre-DI

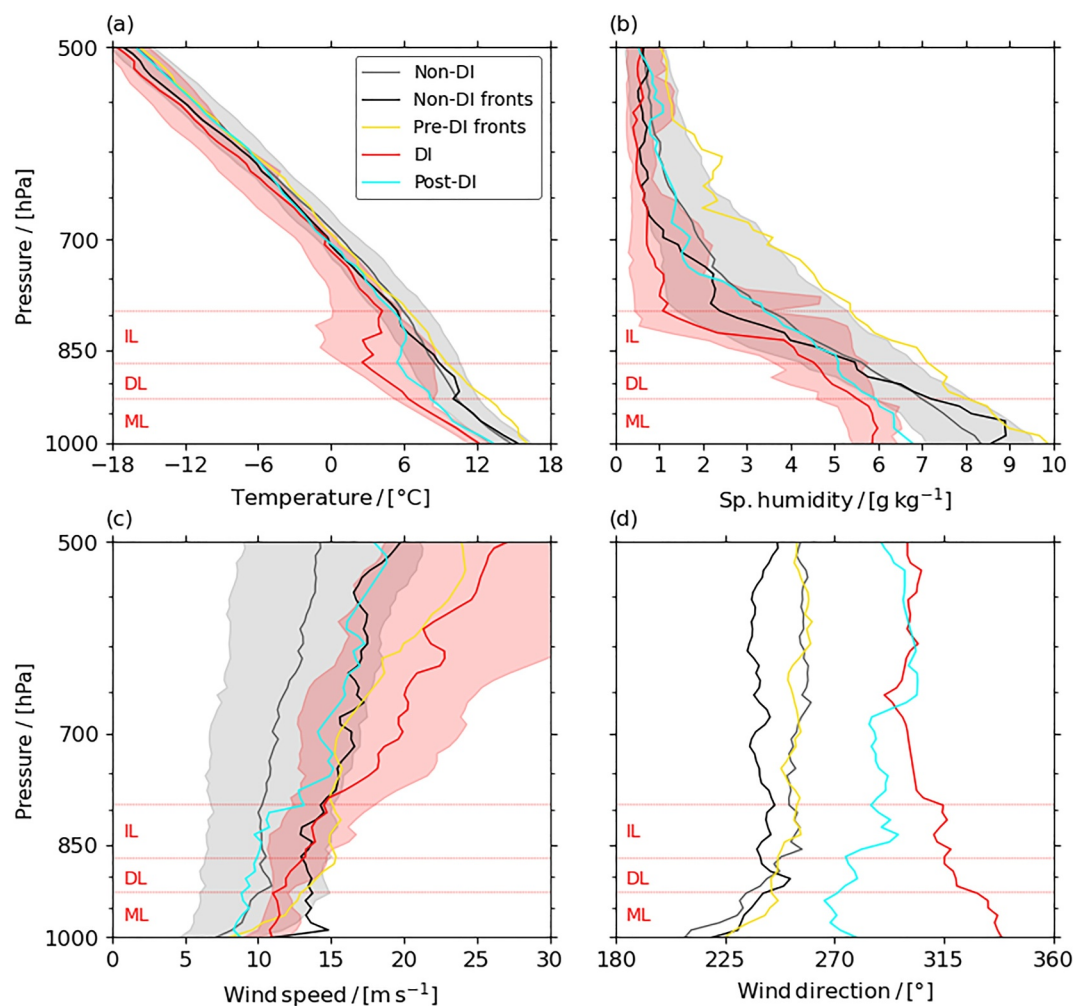


**Figure 1.** Radiosonde profiles of (a) temperature, (b) specific humidity, (c) horizontal wind speed and (d) wind direction ( $360^\circ$  is northerly). Solid lines are median values for each dry intrusion (DI) class and shaded areas mark the interquartile range for Non-DI (gray) and DI (red) class. Median wind speed is the median of the scalar wind speed observations. Median wind direction is the unit vector median wind direction. Dashed red lines show a layer classification for the DI class. IL = inversion layer, DL = decoupled layer; ML = mixed layer.

front, Non-DI fronts) are different in shape, they are characterized by rather low values in the free troposphere. For the moisture innovations (Figure 2b) the Non-DI class has a dry bias up to  $\sim 800$  hPa with a low-level maximum ( $\sim 0.35 \text{ g kg}^{-1}$ ) at  $\sim 925$  hPa. The DI classes differ from the average distribution and among each other. While the moist pre-DI front class exhibits a wet bias ( $\sim -0.4 \text{ g kg}^{-1}$ ) in the lowest 50 hPa, the DI class is characterized by a dry bias of  $\sim 0.5 \text{ g kg}^{-1}$  (8%–10%) in the ML, which is also present but smaller in the post-DI phase, overall suggesting a too-strong humidity contrast across the cold front. Non-DI wind speed bias in the background (Figure 2c), which is positive and increases with altitude and wind speed, exhibits a local maximum ( $0.7 \text{ m s}^{-1}$ ) near the surface. Interestingly, these underestimated wind speeds in the lowest 50 to 80 hPa also occur in all other classes ranging from 1 to  $3 \text{ m s}^{-1}$ . Except for the lowest levels, the highest positive wind speed innovations ( $1\text{--}2 \text{ m s}^{-1}$ , i.e., slow wind bias) occur at 900–700 hPa in the descending DI air. The wind direction background departures for Non-DIs are largest at the surface ( $\sim 5^\circ$ ), and quickly decrease with altitude. Remarkably, the DI class exhibits even higher low-level wind direction innovations of  $-7$  to  $-10^\circ$  (i.e., bias toward more northerly) extending vertically in the ML (Figure 2d). For the Pre-DI front profiles, the near surface wind direction background error is positive ( $\sim 2^\circ$ ), suggesting overall a too large wind direction shift across the cold front in the background forecast caused primarily by the DI side.

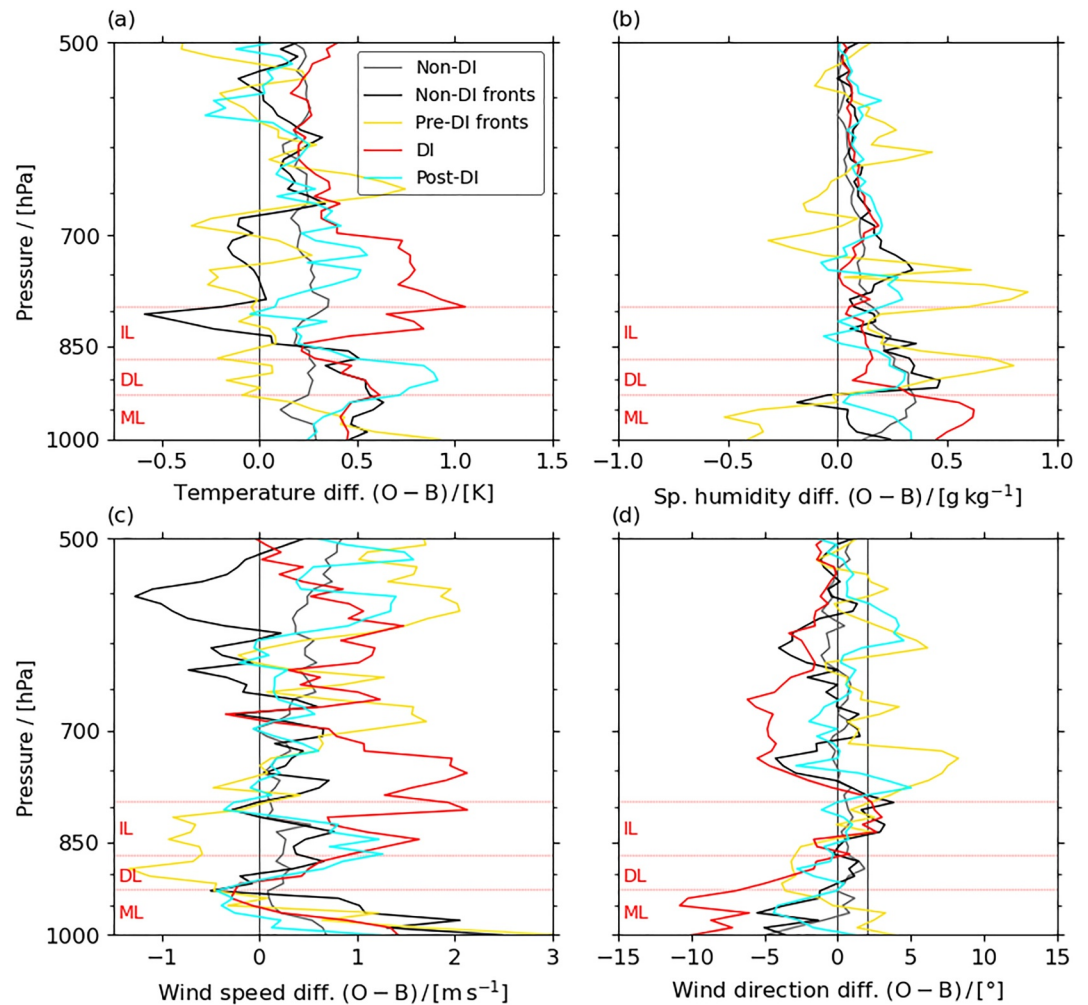


**Figure 2.** Profiles of background departures (O-B, innovation) of (a) temperature, (b) specific humidity, (c) horizontal wind speed and (d) wind direction. Solid lines are median values for each dry intrusion (DI) class. Dashed red lines show a layer classification for the DI class as in Figure 1. IL = inversion layer, DL = decoupled layer; ML = mixed layer; O = observation; B = background.

### 3.3. Analysis Departures

Ideally, DA draws the background forecast toward the observations and reduces the errors in the analysis. The comparison between background and analysis departures (Figure 3) shows that DA overall reduces the biases, however, the influence varies for the different parameters, altitudes and classes. For the Non-DI class small positive temperature innovations are about halved at all altitudes (Figure 3a) and the dry bias almost vanishes above 800 hPa but remains increased in the MBL below ( $\sim 0.25 \text{ g kg}^{-1}$  at  $\sim 940 \text{ hPa}$ ; Figure 3b). The analysis departures (residual) for wind speed (Figure 3c) and direction (Figure 3d) are mostly small as DA reduces the background wind bias above 700 hPa (error reduction of 50%–90%) and the stronger negative wind direction bias at the surface (reduced by  $\sim 80\%$ ). However, the near-surface wind speed underestimation ( $\sim 0.8 \text{ m s}^{-1}$ ) remains in the analysis. For the DI class it can be noted that DA substantially reduces the cold bias in the descending air and the MBL beneath (by  $\sim 60\%$ – $70\%$ , Figure 3m), whereas the dry bias in the ML (Figure 3n) remains almost constant. Analysis winds in the DI class (Figures 3o and 3p) show a significant improvement, however, the underestimated wind speed at the surface does not change, an issue that becomes apparent in all classes.

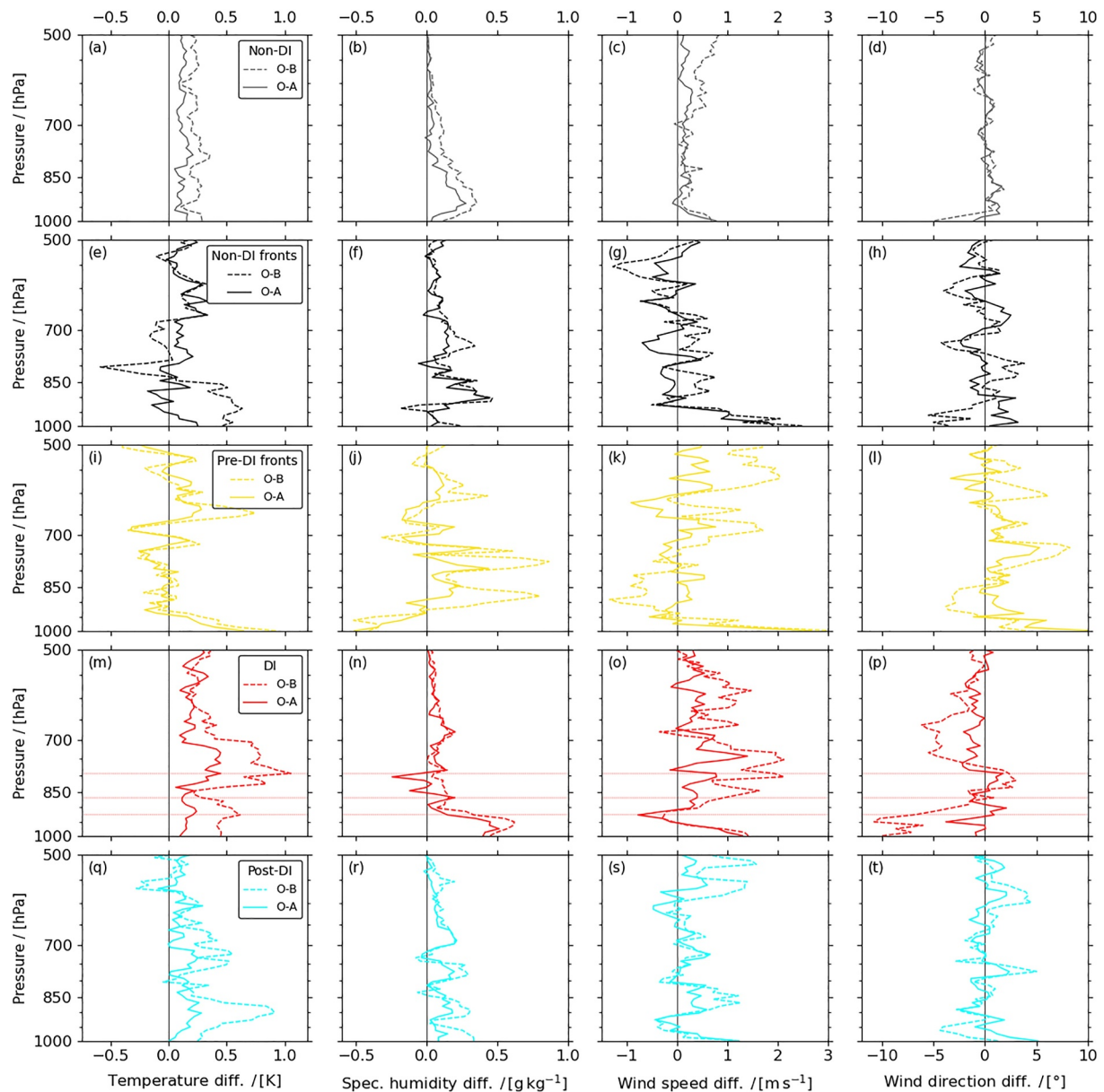


**Figure 3.** Median profiles of background departures (O-B, innovation, dashed lines) and analysis departures (O-A, residual, solid line) for all dry intrusion (DI) classes (Non-DI (a–d, gray), Non-DI fronts (e–h, black), Pre-DI (i–l, yellow), DI (m–p, red), Post-DI (q–t, cyan)) and the variables temperature (a, e, i, m, q), specific humidity (b, f, j, n, r), horizontal wind speed (c, g, k, o, s) and wind direction (d, h, j, p, t). Layer classification (dashed red lines in m–p) as in Figures 1 and 2. O = observation; B = background; A = analysis.

#### 4. Discussion and Conclusions

In this study, the representation of the characteristic sequence of events related to DIs passing over the Azores, as described in Iltoviz et al. (2021), is analyzed in ECMWF's IFS using temperature, humidity and wind data for the observations, background forecast and analysis. Although the once-daily, operationally assimilated 256 radiosonde profiles at Lajes, Terceira Island, Azores in DJF 2016–2018 have a reduced data coverage compared to the 6/12-hourly profiles at Graciosa Island used by Iltoviz et al. (2021), the average profiles are remarkably similar. The comparable profiles and relative shares of each DI class justify the application of the classification to Lajes, which is about 90 km apart from Graciosa.

The analysis of differences between observations and background forecasts (innovation) in comparison with differences to the analysis (residual) allowed biases to be investigated and the influence of DA to be evaluated. The key findings related to the initial research questions (a) and (b) are:

1. The comparison of innovations for the DI class with the Non-DI class representing the average situation indicates a few noticeable differences: Descending DI air, which is located in the IL and above, is characterized by a cold bias, which potentially affects the cold bias in the MBL through vertical mixing (Sandu et al., 2013). The DI cold bias is stronger than the overall positive temperature background bias. The latter agrees with Lavers et al. (2020). In addition, wind speeds are underestimated at the surface. Such a slow surface wind bias was related to underestimated vertical mixing in unstable convective MBLs at noon (Brown et al., 2006). The ML also has a relatively constant dry bias which may be a consequence of the slow wind bias as parameterized moistening through surface latent heat fluxes depends on surface wind speed (ECMWF, 2016b). Although weaker in magnitude, the same combination of a MBL dry bias and near-surface slow wind bias was found in warm advection cases (Lavers et al., 2020). The presented results differ from the overestimated winds in cold air outbreaks over the North Atlantic Gulf stream in ERA5 reanalyses presented by Seethala et al. (2021), which they related to overestimated latent heat fluxes. Surface wind direction background departures of  $-5^\circ$  for Non-DIs agree with findings in Sandu et al. (2020). However, the higher wind direction bias for the unstably stratified MBL during DIs disagrees with studies that find strongest errors in stably-stratified warm advection situations (Brown et al., 2005, 2006). It would be interesting to further evaluate how DIs, which are likely related to exceptionally strong instability at the surface, influence the smaller but more important contribution of cold advection situations to the overall wind direction bias (Sandu et al., 2020). Considering individual wind components (see Figure S5a in Supporting Information S1), almost zero meridional wind bias agrees with Sandu et al. (2020), while the diagnosed small positive zonal bias is opposite. It has to be noted that these differences may be related to the sampling at 12 UTC and, thus, may not be representative for daily averages. And, the lowest pressure level (1,000 hPa) is not exactly corresponding to wind at the surface.
2. In general, the operational assimilation of radiosonde observations is able to reduce errors in the background forecasts efficiently. The DI-related biases are decreased in the analysis, except for the surface wind speed and MBL humidity bias. As both are linked through surface latent heat fluxes, it is hypothesized that the humidity dry bias in the ML is related to the low wind speed bias. Although we find a positive influence of DA at the profile location and it is expected that DA spreads the information in space, the non-local influence of the presented observations on the representation of DI and MBL remains unclear. The Azores are one of the rare global oceanic locations that provide profile data. Other conventional observations are limited to a few buoys and ship observations (Pauley & Ingleby, 2022) and remote sensing data is too coarse and low-resolution to resolve the shallow features presented in this study. Although an influence of such other data types cannot be excluded, the diagnosed influence at Lajes is likely related to the radiosonde observations.

General conclusions about the systematic of the diagnosed errors are limited due to the small number of DI cases observed at noon. However, a height dependent analysis of innovation and residual distributions for the DI class (see Figure S6 in Supporting Information S1 showing the interquartile ranges and a comparison of mean and median values) corroborates the reliability of the sign of the described biases. Certainly, extending the analysis to other years would add more DI cases, but, the NWP system also undergoes changes that influence error statistics (Sandu et al., 2020). The presented results can be considered representative for the Azores and possibly for oceanic regions at the equatorward edge of the storm track for the particular winter months. However, for coastal or land stations, less clear DI average profiles and biases were diagnosed (Sperka, 2024) likely related to the different PBL evolution over land and differing moisture sources. It needs to be mentioned that the presented findings are specific to the ECMWF IFS and other modeling systems may contain different types of errors.

DIs will be a central topic of the North Atlantic Waveguide, Dry Intrusion, and Downstream Impact Campaign (NAWDIC), which is an international research endeavor planned for winter 2025/2026 (<https://www.nawdic.kit.edu>). NAWDIC shall provide airborne profile observations of the DI interacting with the MBL. Surface latent heat fluxes in different parts of the cold sector will be characterized to better understand the connection of moisture and wind biases and their relation to MBL stability. Airborne observations allow the spatial and temporal variability of the biases to be studied in greater detail and to be contrasted with warm air advection ahead of the cold front. Multi-scale observations of processes ranging from parametrized boundary layer processes through large-scale transport will help analyzing the systematics of the presented biases, their correlation and indicated

broader implications for the evolution of mid-latitude weather given by the sensitivity to MBL processes in the cold sector of cyclones (Dacre et al., 2019; Demirdjian et al., 2023).

### Data Availability Statement

The operational DA data is archived in the Meteorological Archival and Retrieval System (MARS) documented at <https://www.ecmwf.int/en/forecasts/access-forecasts/access-archive-datasets> (last access: 18 March 2023). The data access is restricted and subject to ECMWF's license regulations described at <https://www.ecmwf.int/en/forecasts/accessing-forecasts>. The access to the DI classification is described in Ilotoviz et al. (2021).

### Acknowledgments

AO and KK were supported by the Transregional Collaborative Research Center SFB/TRR 165 “Waves to Weather” ([www.wavestoweather.de](http://www.wavestoweather.de)) funded by the German Research Foundation (DFG). The contribution of AO was partly carried out within the Italia—Deutschland science-4-services network in weather and climate (IDEA-S4S, INVACODA, 4823IDEAP6). This Italian-German research network of universities, research institutes and Deutscher Wetterdienst is funded by the BMDV (Federal Ministry of Digital and Transport). The contribution of JQ was partly funded by the European Union (ERC, ASPIRE, 101077260). SRR was partially supported by the European Union (ERC, ExTra, 101075826). The authors thank ECMWF for granting access to the data. We thank Stefan Kaufmann (DLR) for the careful review of the manuscript. Open Access funding enabled and organized by Projekt DEAL.

### References

- Aemisegger, F., & Papritz, L. (2018). A climatology of strong large-scale ocean evaporation events. Part I: Identification, global distribution, and associated climate conditions. *Journal of Climate*, *31*(18), 7287–7312. <https://doi.org/10.1175/JCLI-D-17-0591.1>
- Belmonte Rivas, M., & Stoffelen, A. (2019). Characterizing ERA-Interim and ERA5 surface wind biases using ASCAT. *Ocean Science*, *15*(3), 831–852. <https://doi.org/10.5194/os-15-831-2019>
- Boutle, I. A., Beare, R. J., Belcher, S. E., Brown, A. R., & Plant, R. S. (2010). The moist boundary layer under a mid-latitude weather system. *Boundary-Layer Meteorology*, *134*(3), 367–386. <https://doi.org/10.1007/s10546-009-9452-9>
- Brown, A. R., Beljaars, A., & Hersbach, H. (2006). Errors in parametrizations of convective boundary-layer turbulent momentum mixing. *Quarterly Journal of the Royal Meteorological Society*, *132*(619), 1859–1876. <https://doi.org/10.1256/qj.05.182>
- Brown, A. R., Beljaars, A., Hersbach, H., Hollingsworth, A., Miller, M., & Vasiljevic, D. (2005). Wind turning across the marine atmospheric boundary layer. *Quarterly Journal of the Royal Meteorological Society*, *131*(607), 1233–1250. <https://doi.org/10.1256/qj.04.163>
- Browning, K. A. (1997). The dry intrusion perspective of extra-tropical cyclone development. *Meteorological Applications*, *4*(4), 317–324. <https://doi.org/10.1017/S1350482797000613>
- Carlson, T. N. (1980). Airflow through midlatitude cyclones and the comma cloud pattern. *Monthly Weather Review*, *108*(10), 1498–1509. [https://doi.org/10.1175/1520-0493\(1980\)108<1498:ATMCAT>2.0.CO;2](https://doi.org/10.1175/1520-0493(1980)108<1498:ATMCAT>2.0.CO;2)
- Catto, J. L., & Raveh-Rubin, S. (2019). Climatology and dynamics of the link between dry intrusions and cold fronts during winter. Part I: Global climatology. *Climate Dynamics*, *53*(3), 1873–1892. <https://doi.org/10.1007/s00382-019-04745-w>
- Dacre, H. F., Martínez-Alvarado, O., & Mbengue, C. O. (2019). Linking atmospheric rivers and warm conveyor belt airflows. *Journal of Hydrometeorology*, *20*(6), 1183–1196. <https://doi.org/10.1175/JHM-D-18-0175.1>
- Demirdjian, R., Doyle, J. D., Finocchio, P. M., & Reynolds, C. A. (2023). Preconditioning and intensification of upstream extratropical cyclones through surface fluxes. *Journal of the Atmospheric Sciences*, *80*(6), 1499–1517. <https://doi.org/10.1175/JAS-D-22-0251.1>
- ECMWF. (2016a). IFS Documentation CY43R1 - Part II: Data Assimilation. Retrieved from <https://www.ecmwf.int/en/elibrary/79987-ifs-documentation-cy43r1-part-ii-data-assimilation>
- ECMWF. (2016b). IFS documentation CY43R1 - Part IV: Physical Processes. Retrieved from <https://www.ecmwf.int/en/elibrary/79989-ifs-documentation-cy43r1-part-iv-physical-processes>
- Frassoni, A., Reynolds, C. A., Wedi, N., Bouallègue, Z. B., Caltabiano, A. C. V., Casati, B., et al. (2023). Systematic errors in weather and climate models: Challenges and opportunities in complex coupled modeling systems. *Bulletin of the American Meteorological Society*, *104*(9), E1687–E1693. <https://doi.org/10.1175/BAMS-D-23-0102.1>
- Givon, Y., Keller, D., Pennel, R., Drobinski, P., & Raveh-Rubin, S. (2024). Decomposing the role of dry intrusions for ocean evaporation during mistral. *Quarterly Journal of the Royal Meteorological Society*, *150*(760), 1791–1808. <https://doi.org/10.1002/qj.4670>
- Hollingsworth, A. (1994). Validation and diagnosis of atmospheric models. *Dynamics of Atmospheres and Oceans*, *20*(3), 227–246. [https://doi.org/10.1016/0377-0265\(94\)90019-1](https://doi.org/10.1016/0377-0265(94)90019-1)
- Ilotoviz, E., Ghate, V. P., & Raveh-Rubin, S. (2021). The impact of slantwise descending dry intrusions on the marine boundary layer and air-sea interface over the ARM eastern North Atlantic site. *Journal of Geophysical Research: Atmospheres*, *126*(4), e2020JD033879. <https://doi.org/10.1029/2020JD033879>
- Kazemirad, M., & Miller, M. A. (2020). Summertime post-cold-frontal marine stratocumulus transition processes over the eastern North Atlantic. *Journal of the Atmospheric Sciences*, *77*(6), 2011–2037. <https://doi.org/10.1175/JAS-D-19-0167.1>
- Krüger, K., Schäfler, A., Wirth, M., Weissmann, M., & Craig, G. C. (2022). Vertical structure of the lower-stratospheric moist bias in the ERA5 reanalysis and its connection to mixing processes. *Atmospheric Chemistry and Physics*, *22*(23), 15559–15577. <https://doi.org/10.5194/acp-22-15559-2022>
- Lavers, D. A., Ingleby, B., Subramanian, A. C., Richardson, D. S., Ralph, F. M., Doyle, J. D., et al. (2020). Forecast errors and uncertainties in atmospheric rivers. *Weather and Forecasting*, *35*(4), 1447–1458. <https://doi.org/10.1175/WAF-D-20-0049.1>
- Lavers, D. A., Rodwell, M. J., Richardson, D. S., Ralph, F. M., Doyle, J. D., Reynolds, C. A., et al. (2018). The gauging and modeling of rivers in the sky. *Geophysical Research Letters*, *45*(15), 7828–7834. <https://doi.org/10.1029/2018GL079019>
- Lavers, D. A., Torn, R. D., Davis, C., Richardson, D. S., Ralph, F. M., & Pappenberger, F. (2023). Forecast evaluation of the North Pacific jet stream using AR Recon dropwindsondes. *Quarterly Journal of the Royal Meteorological Society*, *149*(756), 3044–3063. <https://doi.org/10.1002/qj.4545>
- Papritz, L., Aemisegger, F., & Wernli, H. (2021). Sources and transport pathways of precipitating waters in cold-season deep North Atlantic cyclones. *Journal of the Atmospheric Sciences*, *78*(10), 3349–3368. <https://doi.org/10.1175/JAS-D-21-0105.1>
- Pauley, P. M., & Ingleby, B. (2022). Assimilation of in-situ observations. In S. K. Park & L. Xu (Eds.), *Data Assimilation for Atmospheric, Oceanic and Hydrologic Applications* (Vol. 4, pp. 293–371). Springer International Publishing. [https://doi.org/10.1007/978-3-030-77722-7\\_12](https://doi.org/10.1007/978-3-030-77722-7_12)
- Rabier, F., Järvinen, H., Klinker, E., Mahfouf, J.-F., & Simmons, A. (2000). The ECMWF operational implementation of four-dimensional variational assimilation. I: Experimental results with simplified physics. *Quarterly Journal of the Royal Meteorological Society*, *126*(564), 1143–1170. <https://doi.org/10.1002/qj.49712656415>
- Raveh-Rubin, S. (2017). Dry intrusions: Lagrangian climatology and dynamical impact on the planetary boundary layer. *Journal of Climate*, *30*(17), 6661–6682. <https://doi.org/10.1175/JCLI-D-16-0782.1>
- Raveh-Rubin, S., & Wernli, H. (2015). Large-scale wind and precipitation extremes in the Mediterranean: A climatological analysis for 1979–2012. *Quarterly Journal of the Royal Meteorological Society*, *141*(691), 2404–2417. <https://doi.org/10.1002/qj.2531>



- Raveh-Rubin, S., & Wernli, H. (2016). Large-scale wind and precipitation extremes in the Mediterranean: Dynamical aspects of five selected cyclone events. *Quarterly Journal of the Royal Meteorological Society*, *142*(701), 3097–3114. <https://doi.org/10.1002/qj.2891>
- Russell, A., Vaughan, G., & Norton, E. G. (2012). Large-scale potential vorticity anomalies and deep convection. *Quarterly Journal of the Royal Meteorological Society*, *138*(667), 1627–1639. <https://doi.org/10.1002/qj.1875>
- Russell, A., Vaughan, G., Norton, E. G., Ricketts, H. M. A., Morcrette, C. J., Hewison, T. J., et al. (2009). Convection forced by a descending dry layer and low-level moist convergence. *Tellus A: Dynamic Meteorology and Oceanography*, *61*(2), 250. <https://doi.org/10.1111/j.1600-0870.2008.00382.x>
- Sandu, I., Bechtold, P., Nuijens, L., Beljaars, A., & Brown, A. R. (2020). On the causes of systematic forecast biases in near-surface wind direction over the oceans (ECMWF Technical Memorandum No. 866). Retrieved from <https://www.ecmwf.int/en/elibrary/81174-causes-systematic-forecast-biases-near-surface-wind-direction-over-oceans>
- Sandu, I., Beljaars, A., Bechtold, P., Mauritsen, T., & Balsamo, G. (2013). Why is it so difficult to represent stably stratified conditions in numerical weather prediction (NWP) models? *Journal of Advances in Modeling Earth Systems*, *5*(2), 117–133. <https://doi.org/10.1002/jame.20013>
- Savazzi, A. C. M., Nuijens, L., Sandu, I., George, G., & Bechtold, P. (2022). The representation of the trade winds in ECMWF forecasts and reanalyses during EUREC4A. *Atmospheric Chemistry and Physics*, *22*(19), 13049–13066. <https://doi.org/10.5194/acp-22-13049-2022>
- Schäfler, A., Dörnbrack, A., Wernli, H., Kiemle, C., & Pfahl, S. (2011). Airborne lidar observations in the inflow region of a warm conveyor belt. *Quarterly Journal of the Royal Meteorological Society*, *137*(658), 1257–1272. <https://doi.org/10.1002/qj.827>
- Schäfler, A., Sprenger, M., Wernli, H., Fix, A., & Wirth, M. (2023). Case study on the influence of synoptic-scale processes on the paired H<sub>2</sub>O–O<sub>3</sub> distribution in the UTLS across a North Atlantic jet stream. *Atmospheric Chemistry and Physics*, *23*(2), 999–1018. <https://doi.org/10.5194/acp-23-999-2023>
- Seethala, C., Zuidema, P., Edson, J. B., Brunke, M. A., Chen, G., Li, X.-Y., et al. (2021). On assessing ERA5 and MERRA2 representations of cold-air outbreaks across the Gulf Stream. *Geophysical Research Letters*, *48*(19). <https://doi.org/10.1029/2021gl094364>
- Sodemann, H., & Stohl, A. (2013). Moisture origin and meridional transport in atmospheric rivers and their association with multiple cyclones. *Monthly Weather Review*, *141*(8), 2850–2868. <https://doi.org/10.1175/MWR-D-12-00256.1>
- Sperka, C. (2024). *Structure of dry intrusions over western Europe on the basis of observational and model data* (MSc thesis). Karlsruhe Institut für Technologie (KIT). Retrieved from [https://www.imk-tro.kit.edu/5734\\_12635.php](https://www.imk-tro.kit.edu/5734_12635.php)
- Teixeira, J., Stevens, B., Bretherton, C. S., Cederwall, R., Doyle, J. D., Golaz, J. C., et al. (2008). Parameterization of the atmospheric boundary layer: A view from just above the inversion. *Bulletin of the American Meteorological Society*, *89*(4), 453–458. <https://doi.org/10.1175/BAMS-89-4-453>
- Uccellini, L. W., Keyser, D., Brill, K. F., & Wash, C. H. (1985). The Presidents' Day cyclone of 18–19 February 1979: Influence of upstream trough amplification and associated tropopause folding on rapid cyclogenesis. *Monthly Weather Review*, *113*(6), 962–988. [https://doi.org/10.1175/1520-0493\(1985\)113<0962:TPDCOF>2.0.CO;2](https://doi.org/10.1175/1520-0493(1985)113<0962:TPDCOF>2.0.CO;2)
- Wenta, M., Grams, C. M., Papritz, L., & Federer, M. (2024). Linking Gulf Stream air–sea interactions to the exceptional blocking episode in February 2019: A Lagrangian perspective. *Weather and Climate Dynamics*, *5*(1), 181–209. <https://doi.org/10.5194/wcd-5-181-2024>
- Wood, R. (2012). Stratocumulus clouds. *Monthly Weather Review*, *140*(8), 2373–2423. <https://doi.org/10.1175/mwr-d-11-00121.1>
- Young, M. V., Monk, G. A., & Browning, K. A. (1987). Interpretation of satellite imagery of a rapidly deepening cyclone. *Quarterly Journal of the Royal Meteorological Society*, *113*(478), 1089–1115. <https://doi.org/10.1002/qj.49711347803>

## References From the Supporting Information

- Ingleby, B. (2017). An assessment of different radiosonde types 2015/2016 (ECMWF Technical Memorandum No. 807). Retrieved from <https://www.ecmwf.int/en/elibrary/80268-assessment-different-radiosonde-types-20152016>
- Ingleby, B., Pauley, P. M., Kats, A., Ator, J., Keyser, D., Doerenbecher, A., et al. (2016). Progress toward high-resolution, real-time radiosonde reports. *Bulletin of the American Meteorological Society*, *97*(11), 2149–2161. <https://doi.org/10.1175/BAMS-D-15-00169.1>